

Observing the MLT and L-shell dependence of ground magnetic signatures of the ionospheric Alfvén resonator

A. Parent, I. R. Mann, and K. Shiokawa

Abstract: The ionospheric Alfvén resonator (IAR) is a natural resonant cavity in the upper ionosphere that can effectively trap shear Alfvén waves within its boundaries, causing them to form a vertical standing wave pattern. The effects of the IAR are observable as discrete spectral features in ground magnetometer data in the 0.1 to 10 Hz range. To date, many studies of ground magnetic signatures of the IAR have focused on observations over time at a single site. In an attempt to understand the global extent of the resonator, we present results of a preliminary study in which we characterize IAR features across a network of stations, mostly within the Canadian sector. We quantify the evolution of IAR eigenfrequencies at each site by analyzing the variation of harmonic frequency values and discrete harmonic frequency spacing over time, and we present the dependence of these properties on magnetic local time (MLT) and L-shell. From our results it can be seen that IAR signatures observed at sites across a wide range of longitudes have characteristics which are ordered by magnetic local time. The IAR eigenfrequencies typically become apparent between 16 and 18 MLT, in the late afternoon/early evening hours, and then increase in frequency, with discrete harmonics becoming spaced further apart, with increasing MLT. Towards midnight, the rate of frequency increase with MLT/UT is observed to slow, with harmonic frequencies reaching a plateau before in some cases decreasing between midnight and 05 MLT. A potential L-shell effect can also be observed by lining up IAR signature onset times and comparing the average frequency spacing between discrete IAR harmonics. The lowest L-value station exhibits the smallest average harmonic frequency spacing and the lowest and most linear rate of increase in harmonic frequency spacing with time. Plans for future work involve further observational studies of IAR magnetic signatures, which will be important in improving our understanding of the physics of the ionospheric Alfvén resonator and its effect upon magnetosphere-ionosphere interactions.

Key words: ionosphere, magnetosphere-ionosphere coupling, ULF waves.

1. Introduction

The ionospheric Alfvén resonator (IAR) is a resonant cavity that is believed to form in the upper ionosphere between two regions of large Alfvén velocity gradients [e.g., 1, 3, 6]. It is thought to be stimulated by the generation of shear Alfvén waves in the E-layer, which may be triggered by electromagnetic emissions due to thunderstorm activity [1, 8], or possibly by fluctuations in the E-region neutral wind [7]. The Alfvén waves, traveling along geomagnetic field lines, can undergo partial reflection at velocity gradients, leading to a vertical standing wave pattern in the upper ionosphere within the resonant cavity (see e.g., papers in a special IAR-related issue of the *Journal of Atmospheric and Solar-Terrestrial Physics*, Vol.62, No.4, March 2000).

The excitation of the IAR can be observed as distinct spectral features in ground magnetometer data in the 0.1 to 10 Hz range. This frequency range includes Pc1-2 geomagnetic pulsations (0.1 to 5 Hz) within the ULF band [5], and extends into lower frequencies of the ELF band. We characterize IAR features occurring over one day, September 25, 2005, across a

collection of magnetometer stations predominantly in the Canadian sector. We quantify the evolution of IAR eigenfrequencies by determining discrete harmonic frequency values and the average frequency spacing between adjacent harmonics as a function of time at each site. This preliminary study allows us to investigate procedures that can be used to quantify IAR resonance features in ground magnetic data. These are the first steps towards performing more in-depth observational studies of the resonator. Ultimately, by characterizing the variation of IAR features with L-shell and magnetic local time, we hope to better understand how the observed IAR features might be used to monitor in real-time the local structure of the topside ionosphere above a point of observation (i.e., a ground magnetometer site).

2. Data Analysis

2.1. Search Coil Magnetometer Network

The network of search coil magnetometer instruments used in the September 25, 2005, study is shown in Figure 1. Four of the stations used are located in Canada, while a fifth (UZR) is located near Lake Baikal in Russia. Station details, including coordinate locations, L-values and instrument information, are summarized in Table 1. The 10 Hz instruments at PKS, HRP, LCL and UZR are remnants of the Solar-Terrestrial Energy Program (STEP) Polar Network that operated between 1991 and 1997. For more information, refer to the website:

Received 28 May 2005.

A. Parent and I. R. Mann. Department of Physics, University of Alberta, Edmonton, AB, T6G2J1, Canada. (aparent@phys.ualberta.ca)

K. Shiokawa. Solar-Terrestrial Environment Laboratory, Nagoya University, Toyokawa 442-8507, Japan.

<http://www-space.eps.s.u-tokyo.ac.jp/hayashi/>. The 64 Hz instrument at ATH is operated by the Solar-Terrestrial Environment Laboratory (STELAB) and is housed by Athabasca University Geophysical Observatory. ATH station information can be found on the website: <http://stdb2.stelab.nagoya-u.ac.jp/index/canada.html>.

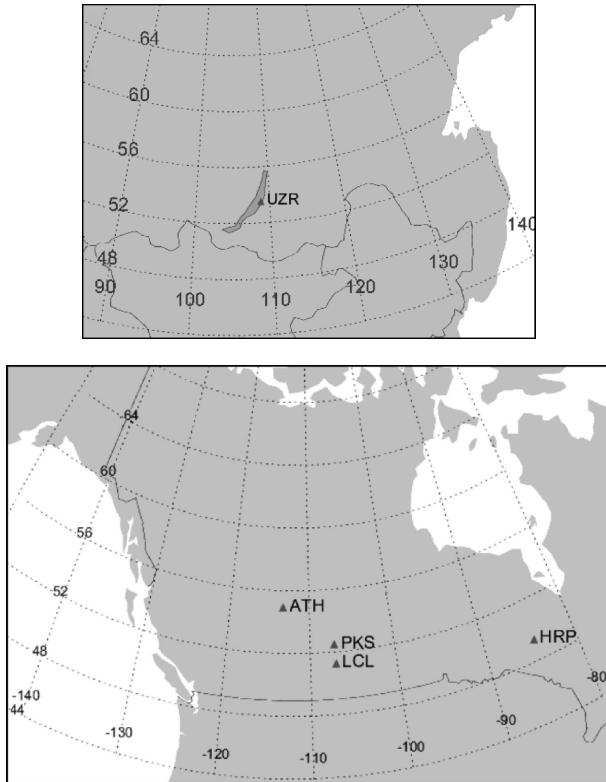


Fig. 1. Search coil magnetometer locations in Russia (top) and Canada (bottom). The grid shows lines of geographic latitude and longitude.

Station	CGM		L-value	Magnetometer Info. Cadence, Available Axes
	Lat	Long		
ATH, Athabasca	62.0	306.6	4.61	64 Hz, H and D
PKS, Parksite	60.7	315.3	4.23	10 Hz, D only
HRP, Hornepayne	59.7	348.1	4.00	10 Hz, D only
LCL, Lucky Lake	59.5	315.7	3.94	10 Hz, H and D
UZR, Uzur, Russia	48.37	181.94	2.30	10 Hz, H and D

Table 1. Summary of search coil magnetometer station locations and relevant instrument details.

2.2. Dynamic Spectra Visualizations of the IAR

Signatures of the IAR, observed in the dynamic power of the D-component (magnetic east-west direction) at each site on September 25, 2005, are shown in Figures 2 and 3 as a function of Universal Time (UT) and magnetic local time (MLT), respectively. The plots from each station listed in Table 1 are shown from top to bottom with decreasing L-value. Data from

the 10 Hz induction magnetometer stations (PKS, HRP, LCL, UZR) was processed using a sliding FFT Hanning window, with a length of 2000 points and a 250 point time step. The 64 Hz induction data from ATH station was processed with a Hanning window length of 12800 points and a 1600 point time step. For all stations, a uniform frequency resolution of 5 mHz and time resolution of 25 seconds were hence obtained.

The IAR signatures are easily identified as the upward sloping, stripe-like structures in the dynamic power spectrograms of Figures 2 and 3. The signatures shown are quite typical of magnetic observations of the resonator [e.g., 2, 3, 9]. Multiple resonance bands (discrete harmonics) generally become visible in the early evening (local time) and increase in frequency, with harmonics becoming spaced further apart, towards local midnight. In some observations of the IAR, harmonics can be seen to decrease in frequency and become spaced closer together as local time progresses from midnight into early morning [9]. Some evidence of this tendency can be seen in the signatures of ATH, PKS and LCL stations, between 00 and 05 MLT in Figure 3.

In Figure 2, in which dynamic power has been plotted as a function of UT, IAR signatures in the ATH, PKS and LCL plots are the most distinctive. Exact onset times are difficult to determine since the discrete banded structure emerges only gradually from the background noise. However, the signatures at these three sites appear to become visible at roughly the same time, around 01 UT, on September 25. This is not surprising, as these stations are located within a small range of longitude (about 10 degrees), and would be rotating into local evening hours at roughly the same UT. It is also interesting to note that in the case of these stations, the power in the discrete frequency signatures of the IAR as compared to background noise (the modulation depth), is observed to increase significantly around 02 UT. IAR features at HRP station are quite diffuse in comparison, with eigenfrequencies difficult to distinguish from the noise, representing a low modulation depth. We would expect IAR signatures at HRP to become visible at an earlier UT, since the station is located about 30 degrees east of the ATH, PKS and LCL stations. However, this is not the case, and the IAR signatures at HRP actually seem to appear at a later UT than they do for the other three stations. Finally, in Figure 2, the UZR station signatures are seen to occur at a much later UT than at any of the other stations. This makes sense since the longitudinal location of the site is very different from the Canadian sector stations. In the course of Universal Time, the Canadian stations rotate into evening first, and the IAR signatures seen during the nighttime at these sites are, in this study, being compared to the IAR signatures seen at the Russian site as UZR rotates hours later into the evening sector. The UZR signatures appear for a much smaller time interval than those seen at the other stations in the Canadian sector.

In Figure 3 essentially the same signatures are displayed, however, their evolution has been plotted as a function of magnetic local time. Most importantly, the signatures for all stations shift in time (from Figure 2 to Figure 3) and become distinct in the late afternoon/early evening hours of MLT, between 16 and 18 MLT. The biggest movement of IAR signatures occurs for UZR station, which shifts from an onset at about 11 UT in Figure 2 to 18 MLT in Figure 3. It is evident then, that for this day at least, as the stations rotate into the evening sec-

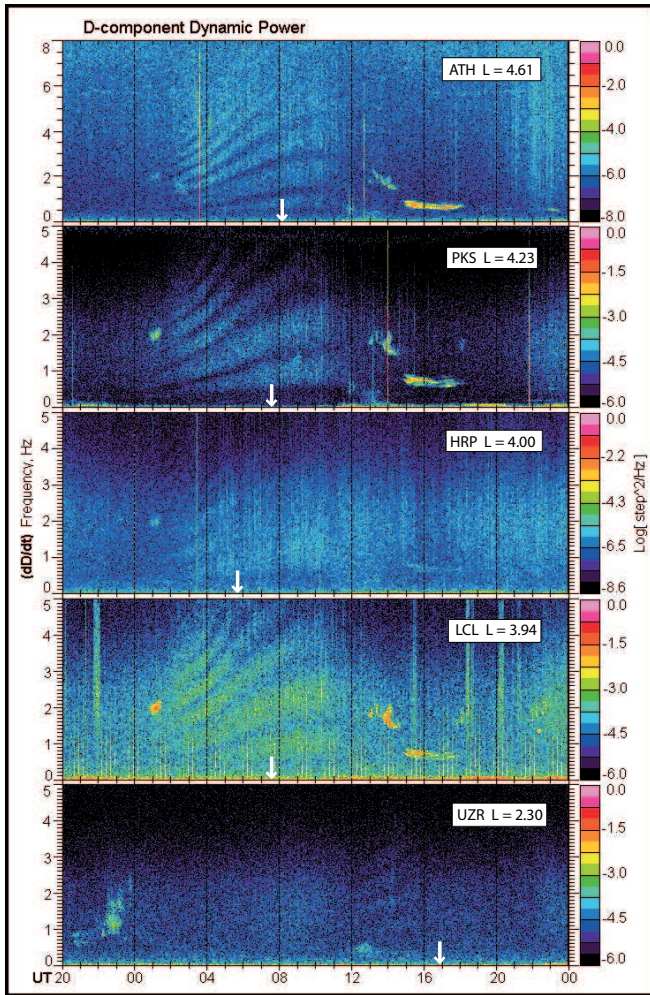


Fig. 2. Dynamic power spectrograms of dD/dt as measured by the magnetometer stations listed in Table 1, in order of decreasing L-shell, as a function of UT. Frequency in Hz is displayed along the ordinate axes, while the abscissa indicates hours of Universal Time, starting at 20 UT on September 24 and running until 00 UT on September 26, 2005. The color-scale represents logarithmic power in arbitrary units. White arrows indicate UT points of local midnight (00MLT). For data processing details, see the text.

tor, the IAR signatures appear in ground magnetic data. This represents a significant MLT effect, indicating that IAR characteristics can be organized by MLT over an extended range of longitudes.

In examining the plots of Figure 3, there appears to be evidence for an L-shell effect as well. The higher L-shell stations (ATH, PKS, HRP and LCL) are perhaps too close in L to exhibit an observable difference when the dynamic power plots are compared by eye. However, the signatures at UZR station, occurring at a significantly lower L-value, appear to exhibit visible differences. The harmonic frequency bands are narrower in frequency and more closely spaced together. Furthermore, the signatures exhibit a less steep slope and evolve in a more linear fashion as time progresses. A more quantitative analysis is presented below and will serve to better measure the differences and similarities of the IAR features at these sites.

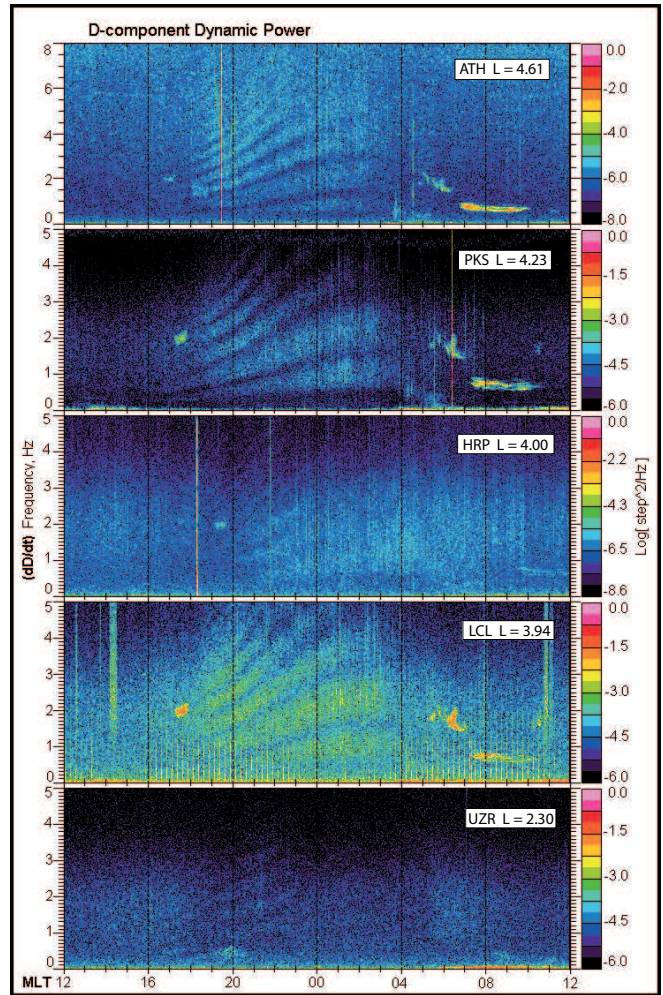


Fig. 3. IAR resonance features in the dynamic power spectrograms of dD/dt as a function of MLT. Frequency in Hz is shown along the ordinate axes. In the top four panels, the 24 hours of MLT (displayed along the abscissa) were formed using data from the UT days: September 24 and 25, 2005. The bottom panel was formed from the UT days: September 25 and 26, 2005. Magnetic data was processed in the same way as in Figure 2; see text for details.

2.3. Quantifying IAR Signatures

A technique based upon the ‘interactive on-screen cursor click’ technique of [4] was used to quantify IAR signatures in this study. IAR harmonics were identified by clicking on the magnified dynamic spectra. An illustration of the technique applied to ATH station data is shown in Figure 4. The identified frequency values for each harmonic were then plotted as a function of time, as in Figure 5. This method exploits the fact that the human eye is an excellent natural filter. It yielded harmonics which were very consistent with dynamic spectra visualizations.

3. Results: IAR Eigenfrequency Evolution

The variation of discrete harmonic frequency values with magnetic local time is shown in Figure 6. In each panel, frequency values for a specific harmonic number, N , are plot-

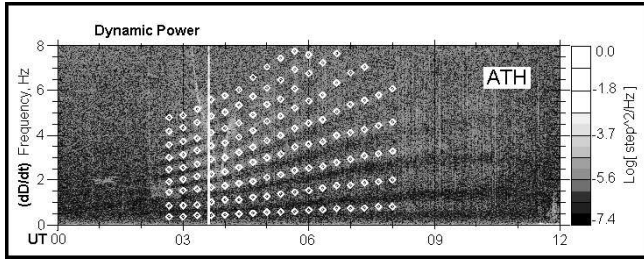


Fig. 4. Harmonic frequency values were determined by clicking on the displayed dynamic power plot. White diamonds indicate where eigenfrequency values were identified with a cursor click. This example shows dD/dt dynamic power spectra for ATH station on 25 September, 2005.

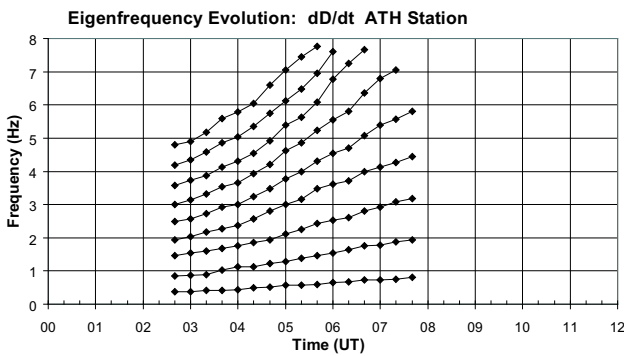


Fig. 5. The evolution of resonance features is thus quantified by plotting eigenfrequency values as a function of time. The plot shows results for ATH station on 25 September, 2005. The time resolution is 20 minutes.

ted for all stations that exhibited the harmonic. The plots are ordered by increasing harmonic number from bottom to top. The precise pinpointing of IAR signature onset times is a delicate task involving the local signal to noise response of the instrument, and the comparison of relative power at discrete IAR eigenfrequencies as compared to power at adjacent frequencies. In this preliminary study, it is important to note that the onset times as shown in Figure 6 are only roughly estimated by eye. In future studies, a more systematic determination of IAR signature onsets may allow onset times to be compared with, for example, ionospheric sunrise/sunset times (at different ionospheric layer heights) to determine if a relationship can be observed.

Consider first the fundamental frequency values plotted in the bottom panel of Figure 6. For all stations, the approximate onset times occur between 16 and 18 MLT, confirming the MLT effect observed and discussed in Section 2.2. In addition, the turning points, where the upward-sloping discrete harmonics are seen to flatten out and begin to slope downward, occur for all sites between 00 and 03 MLT. The observations at these sites on this particular day suggest that IAR signatures can be organized according to magnetic local time regardless of longitudinal location, as their onset times tend to become aligned in the late afternoon/early evening MLT hours, and their turning points tend to become aligned around midnight/early morning MLT.

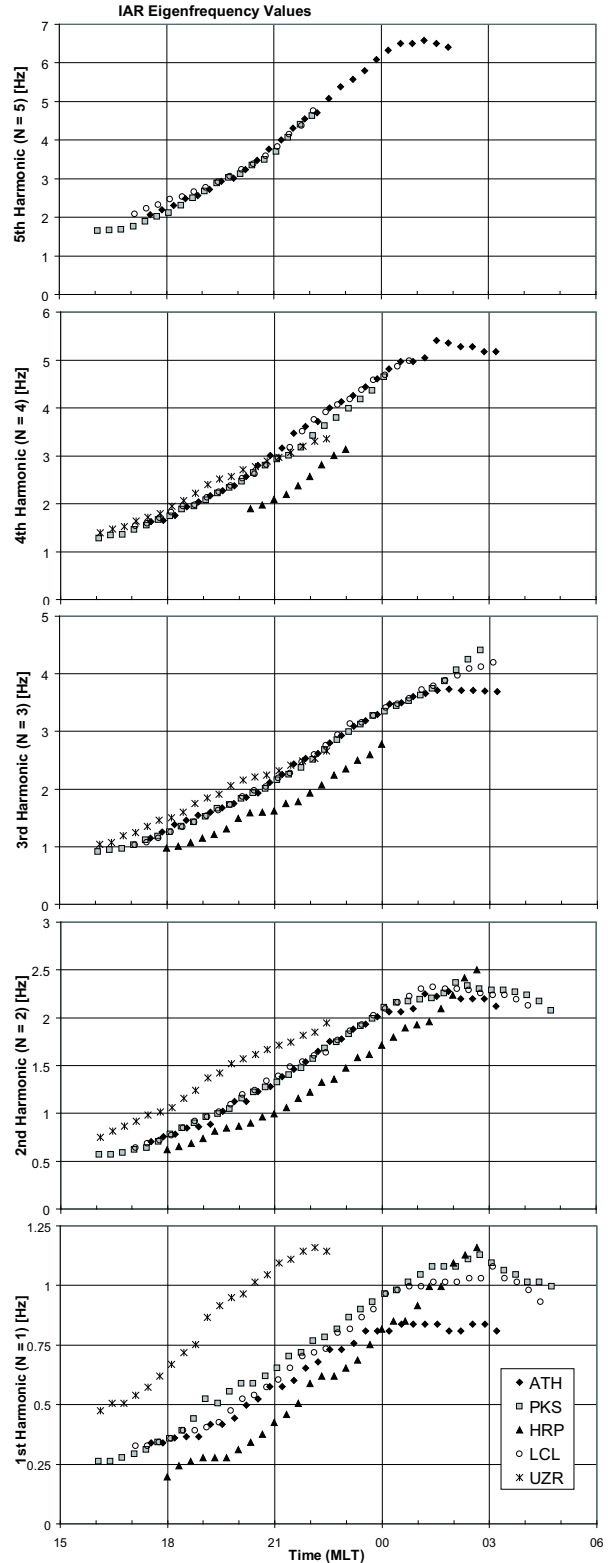


Fig. 6. Variation of harmonic frequency values with magnetic local time, as determined from analysis of dD/dt dynamic power spectra. In each panel, frequency values of a specific harmonic number, N, are plotted for each station. Stations and corresponding symbols are indicated in the legend.

In Figure 6, the lowest harmonic ($N = 1$) eigenfrequencies at PKS and LCL behave very similarly, as might be expected since these sites are located close to each other and their local ionospheres may share comparable characteristics. The fundamental harmonic at ATH starts off like that of PKS and LCL, however the positive gradient signature flattens out at a lower frequency value. The stations at HRP and UZR exhibit more unique IAR behavior with respect to the fundamental frequency. The fundamental mode harmonic at HRP shows the lowest frequency values of all the stations, while at UZR, the first harmonic consists of the highest frequency values. It should be noted that the identification of this harmonic as the fundamental one, in the case of UZR station, was very difficult, owing to the large amount of magnetic activity in the Pc1 range occurring around 18 – 21 MLT.

Regarding the higher order harmonics displayed in Figure 6, the discrete IAR eigenfrequencies at each site behave, in relation to one another, very much as they did in the fundamental frequency case. For $N > 1$, IAR signatures at ATH follow more closely the behavior of signatures at PKS and LCL. As N increases, HRP continues to exhibit the lowest harmonic frequency values. At $N = 3$ and 4, the eigenfrequencies at UZR decrease, approaching those of ATH, PKS and LCL stations, however it can also be seen that the UZR signatures display a slightly less steep slope as frequency values increase with MLT. Finally, in the $N = 5$ plot, it becomes too difficult to quantify higher harmonic frequency values for UZR and HRP stations. The fifth harmonics at PKS, ATH and LCL behave in a similar manner.

In addition to considering absolute frequency values of IAR harmonics at each site, it is also of interest to calculate the average frequency spacing between adjacent harmonics as a function of time. This quantity, sometimes referred to as frequency scale, effectively describes how spread apart, on average, the discrete eigenfrequencies are, and its time dependence indicates how the spreading evolves (e.g., linearly or non-linearly) and at what rate. In Figure 7, the evolution of harmonic frequency spacing is presented as a function of MLT. The general IAR trend involving an increase in frequency scale over time towards midnight, and then a decrease into the early morning hours is observed here. The frequency spacing of the ATH, PKS and LCL signatures initially evolve in a similar manner, from 17 - 22 MLT. After this time, the frequency scales deviate. The harmonic spacing at ATH increases quickly between 22 and 23 MLT, and then its positive gradient lessens gradually until, from 02 - 03 MLT, a decrease in spacing occurs. Beyond 22 MLT, the frequency spacing at PKS and LCL increase fairly linearly until abrupt drop-offs at about 03 MLT. The discontinuous drop-offs in frequency scale are artifacts of the disappearance of quantifiable upper harmonics that are significantly spread out in frequency. The subsequent decrease in frequency scale at PKS and LCL indicates that the eigenfrequencies become more closely spaced together as they decrease in frequency into the early morning hours of MLT.

The average frequency spacing between IAR harmonics is at all times the lowest at HRP and UZR. In comparing these two stations at each MLT in Figure 7, it is clear that on average the discrete IAR harmonics are closer together at HRP than they are at UZR. Consider now another plot of the average harmonic frequency spacing at each station, shown in Figure 8. In

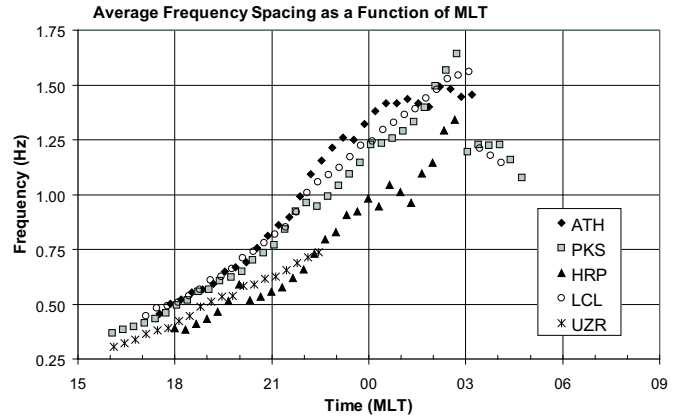


Fig. 7. Average frequency spacing between adjacent IAR harmonics at each station, as a function of MLT. The legend indicates stations and corresponding symbols.

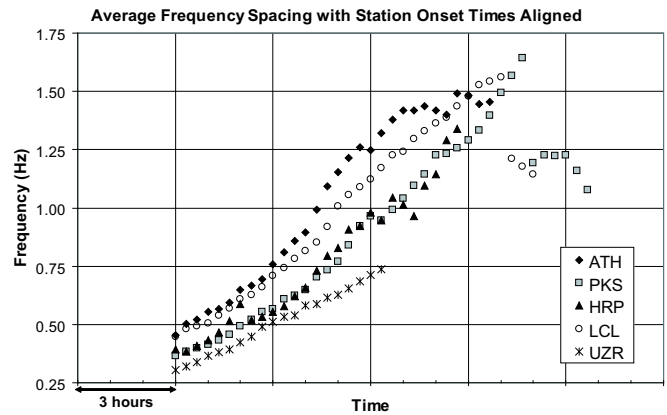


Fig. 8. Average frequency spacing between adjacent IAR harmonics with signature onset times at all stations lined up. The data series shown in Figure 7 have essentially been shifted in time so their first data points coincide. The abscissa indicates time intervals during the evolution of eigenfrequencies and does not indicate specific MLT or UT instances. See text for more details.

this figure, the onset times of the IAR signatures at each site have been lined up to coincide with each other. This allows the evolution of frequency scales to be compared from a common starting point (onset time), regardless of when, in MLT, the signatures at each site actually occurred. Hence, the frequency scales plotted in Figure 7 have been shifted in time in Figure 8, so that their first data points occur simultaneously at an arbitrary time. Note that as a result the abscissa in Figure 8 indicates general time intervals only, essentially measuring the evolution of IAR signatures from the moment they become apparent in magnetic data (exhibit onset). The time axis does not indicate specific MLT or UT instances. In Figure 8, it can be seen that UZR station exhibits the lowest average frequency spacing as harmonics evolve. Compared to the other stations in Figure 8, UZR also demonstrates the lowest increase in frequency scale from onset time until its IAR signatures disappear, as well as the most linear increase in frequency scale during this time

period. UZR is the lowest L-shell station, with an L-value of 2.30, and it may be possible that Figure 8 is revealing the L-shell effect that was more qualitatively observed in Section 2.2. The harmonic frequency spacing at ATH, which is the highest L-shell station with $L = 4.61$, exhibits the highest frequency values, the sharpest increase over time and the most non-linear trend. The frequency scales of the intermediate L-value stations, PKS, HRP and LCL, do not show a clear ordering of behavior according to L-value in Figure 8. But the differences on average between the higher L stations, in particular, ATH, and the lowest L station, UZR, are marked. This L-shell effect has been reported in previous studies of the IAR, in which high and low L observations have been compared [e.g., 3]. It has typically been found that at lower L-shell stations, as compared to higher L stations, the average frequency spacing between adjacent harmonics is lower and does not exhibit as much of a dependence on local time from the early evening into the night hours.

4. Summary

A preliminary investigation of ground magnetic signatures of the ionospheric Alfvén resonator has been conducted on September 25, 2005, across a network of five search coil magnetometer sites. This preliminary study has allowed us to explore and evaluate methods that can be used to quantify IAR resonance features in ground magnetic data. We have determined that a visual on-screen determination of eigenfrequencies is a reasonable and promising quantification technique. General observations of IAR features are consistent with the results of previous studies. In particular, we have found that when IAR signatures, observed at sites spread across a range of longitudes, are organized by MLT, their onsets tend to become aligned, occurring within a few hours of each other in MLT. The IAR eigenfrequencies emerge from the background noise between 16 and 18 MLT, in the late afternoon/early evening hours, and initially increase in frequency, with harmonics becoming spaced further apart, over time. At some sites, the harmonic frequencies are observed to plateau and then subsequently decrease in frequency between midnight and 05 MLT. There is also evidence for an L-shell effect when the average frequency spacing between discrete IAR harmonics is displayed, this being especially clear when IAR signature onset times at different stations are made to coincide. The lowest L-value station exhibits the smallest average frequency spacing and the lowest and most linear rate of increase in harmonic frequency spacing over time.

Future work involving the IAR will consist of the analysis of magnetic signatures over a longer time interval and a larger network of stations. This will allow us to quantify the occurrence rates of IAR excitation and better analyze the dependence of the properties of IAR features on MLT, L-shell, sunrise/sunset times and geomagnetic activity level. We are also interested in examining the relationship between structured Pc1-2 pulsations and resonant IAR eigenfrequencies. Overall, this research effort has provided a solid foundation for future studies to build upon. Expanded studies will ultimately enable us to explore the global character of the spectral features of the ionospheric Alfvén resonator, and the extent to which

observed IAR characteristics can be used as a real-time monitor of the structure of the topside ionosphere.

Acknowledgments: PKS, LCL, HRP and UZR station magnetometer data were provided by Kanji Hayashi. The ATH search coil magnetometer is housed at the Athabasca University Geophysical Observatory. This work was supported by a Canadian NSERC Discovery Grant to I.R.M.

References

1. Belyaev, P. P., Polyakov, S. V., Rapoport, V. O. and Trakhtengerts, V. Yu., The ionospheric Alfvén resonator, *Journal of Atmospheric and Terrestrial Physics*, 52, 781, 1990.
2. Belyaev, P. P., Bosinger, T., Isaev, S. V. and Kangas, J., First evidence at high latitudes for the ionospheric Alfvén resonator, *Journal of Geophysical Research*, 104, 4305, 1999.
3. Bosinger, T., Haldoupis, C., Belyaev, P. P., Yakunin, M. N., Semenova, N. V., Demekhov, A. G. and Angelopoulos, V., Spectral properties of the ionospheric Alfvén resonator observed at a low-latitude station ($L=1.3$), *Journal of Geophysical Research*, 107, 1281, 2002.
4. Hebden S. R., Robinson T. R., Wright D. M., Yeoman T., Raita T. and Bosinger T., A quantitative analysis of the diurnal evolution of ionospheric Alfvén resonator magnetic resonance features and calculation of changing IAR parameters, *Annales Geophysicae*, 23, 1711, 2005.
5. Jacobs, J. A., Kato, Y., Matsushita, S. And Troitskaya, V. A., Classification of geomagnetic micropulsations, *Journal of Geophysical Research*, 69, 180, 1964.
6. Lysak, R. L., Generalized model of the ionospheric Alfvén resonator, in: Auroral Plasma Dynamics, Geophysical Monograph 80, American Geophysical Union, 121, 1993.
7. Surkov, V. V., Pokhotelov, O. A., Parrot, M., Fedorov, E. N. and Hayakawa, M., Excitation of the ionospheric resonance cavity by neutral winds at middle latitudes, *Annales Geophysicae*, 22, 2877, 2004.
8. Surkov, V. V., Molchanov, O. A., Hayakawa, M. and Fedorov, E. N. Excitation of the ionospheric resonance cavity by thunderstorms, *Journal of Geophysical Research*, 110, A04308, 2005.
9. Yahnin, A. G., Semenova, N. V., Ostapenko, A. A., Kangas, J., Manninen, J. and Turnunen, T. Morphology of the spectral resonance structure of the electromagnetic background noise in the range of 0.1-4 Hz at $L = 5.2$, *Annales Geophysicae*, 21, 779, 2003.